Influence of rigid side chain attraction on stiffness and conformations of comb copolymer brushes strongly adsorbed on a flat surface

Flikkema, E; ten Brinke, G.

Published in:
Macromolecular Theory and Simulations

DOI:
10.1002/1521-3919(20020901)11:7<777::AID-MATS777>3.0.CO;2-A

Full Paper: The influence of side-chain attraction on the conformational properties of two-dimensional polymer brushes with rigid side chains is investigated using Monte Carlo simulations. Using a rigid backbone, a characteristic interaction strength is determined by investigating the critical interaction energy for the collapse of the side chains onto the backbone. For a flexible backbone, the persistence length of the backbone is found to decrease with increasing attraction, irrespective of whether side-chain flipping is allowed or not. This result is in good agreement with the theoretical modeling presented before. If side-chain flipping is allowed, the attraction between the side chains leads to aggregation of successive side chains at one side of the backbone resulting in a characteristic local spiraling of the backbone.

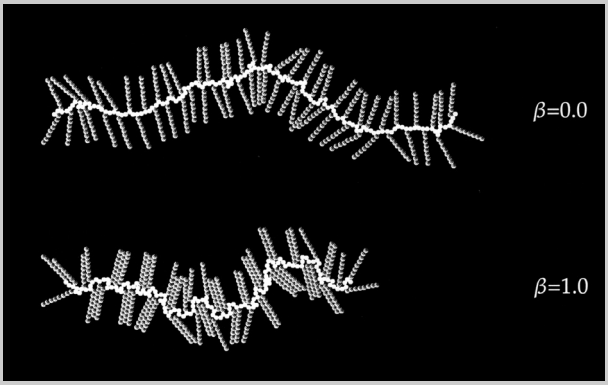

Snapshots of polymer brushes consisting of a flexible backbone of 128 beads with every other bead carrying a rigid side chain of 8 beads pointing alternately to opposite directions of the backbone. Besides the excluded-volume interaction between all beads, the side-chain beads attract each other via a potential $V(r) = -\varepsilon/r^6$ and the snapshots correspond to different values of $\beta = \varepsilon/kT$.

Influence of Rigid Side Chain Attraction on Stiffness and Conformations of Comb Copolymer Brushes Strongly Adsorbed on a Flat Surface

E. Flikkema, G. ten Brinke

Laboratory of Polymer Chemistry, Materials Science Centre, University of Groningen, Nijenborgh 4, 9747 AG Groningen, The Netherlands

Keywords: conformational analysis; graft copolymers; Monte Carlo simulation

1 Introduction

The conformational characteristics of comb copolymers with a high grafting density of side chains has been addressed in a series of theoretical papers[1–10] beginning with the original work of Birshtein et al.[1] Irrespective of whether a good solvent or a θ-solvent is used, all theories predict cylindrical brush-like structures for sufficiently long side chains. The pertinent parameters are the side-chain grafting density σ, the side chain length M, the intrinsic stiffness of the backbone and the side chains and the solvent quality with respect to the side chains and the backbone. The conformation is characterized by a number of parameters of which the persistence length λ of the comb copolymer backbone, the diameter D of the cylindrical structure and the *spatial* distance l between the grafting points are most important. The theoretical studies all demonstrate that for sufficiently long flexible side chains the persistence length will exceed the backbone length, thus resulting in a characteristic cylindrical "bottle-brush" structure. An explicit expression for the persistence length was first derived by Fredrickson[3] as $\lambda/D \propto M^{9/8}\sigma^{17/8}$. Furthermore, the backbone *expands* locally, however, the dependence of l on the side chain length M is relatively weak.

Subsequent computer simulations using a freely jointed hard sphere model failed to confirm one essential aspect of this picture.[11–16] Whereas both D and l indeed increased as a function of M, λ/D appeared to be independent of the side-chain length up to $M = 80$.[11] This apparent inconsistency is now believed to arise from the

  1022-1344/2002/0709–0777$17.50+.50/0

fact that extremely long side chains are required to enter the scaling regime. The conformation of the side chains can be described as a series of blobs of increasing size.[1–3] The scaling of the persistence length is related to the number of blobs rather than to the number of monomers and thus difficult to reach by computer simulations.

This problem can be circumvented using rigid rather than flexible side chains, a problem that was first addressed in a paper by Subbotin et al.,[6] where the following scaling relations were derived: $\lambda/D \propto M$, $l \propto M^0$. The most striking difference between these predictions and those involving the flexible side chains is the side-chain-length dependence of the spatial distance l between successive grafting points. In the case of flexible side-chains l is predicted to increase with increasing side-chain length, an extension confirmed by computer simulations. In the case of rigid side chains, on the other hand, l is predicted to be approximately independent of the side chain length. The latter result was also shown to be in excellent agreement with computer simulations; locally the backbone conformation continues to fluctuate strongly, independent of the length of the rigid side chains. Computer simulations involving rigid side chains indeed confirmed the strong increase of λ/D with M theoretically predicted. An important conclusion from these simulations is that stiff side chains are far more effective stiffness inducing moieties than flexible side chains. This was further verified in a computer simulation study in which the stiffness of the side chains was varied systematically.[16]

The experimental investigation of comb copolymers with a high grafting density has assumed large proportions after the successful polymerization of macromonomers, by Tsukahara and coworkers.[17–20] Besides polymerization of macromonomers alternative routes have been developed recently using grafting from a macroinitiator prepared by either atom-transfer radical polymerization[21] or by living cationic polymerization.[22] The experimental characterization of the comb copolymer brush conformation in dilute solution is a highly nontrivial issue. It was achieved by Schmidt and co-workers[23–30] using a combination of light-scattering experiments and theoretical modeling. They demonstrated how to determine the length l per vinylic main chain monomer from the experimentally accessible form factor $P(q)$ using a so-called Holtzer plot. For high-molar-mass polymacromonomers based on methacryloyl end-functionalized oligo methacrylates ($\overline{M}_n$ = 2410 g/mol) in the good solvent tetrahydrofuran, the length l per vinylic main chain monomer was found to be 0.071 nm per monomer, compared to 2.5 nm for a fully all-*trans* chain. The Kuhn statistical segment length l_k (= 2λ) turned out to be 120 nm. These results compare favorably with the computer simulation results for semiflexible side chains. In particular the fact that the length of the worm-like cylinder per vinylic main chain monomer is considerably smaller than the all-*trans* value is qualitatively in excellent agreement with the simulation data. The persistence length of the cylindrical comb copolymer structure of the real molecules is expected to be somewhat larger than observed in the computer simulations, since the latter involved a completely flexible backbone.

All the results mentioned so far concern three-dimensional solutions of comb copolymer molecules. However, the scanning force microscopy applied extensively to image these molecules obviously probes their two-dimensional structure.[27,30–32] The pictures demonstrate the worm-like nature of the conformations, which can be analyzed in terms of the same quantities as used to characterize the dilute solution conformations. However, in view of the influence of the two-dimensional (2d) confinement, the interaction with the substrate as well as the influence of the casting process itself, the results will strictly speaking only be meaningful for the 2d situation itself. In particular, because the excluded-volume effect is so much stronger, a comb copolymer brush adsorbed on a flat surface will appear to be much stiffer than in a bulk solvent.[14] Furthermore, topological constraints, not present in the 3d case, may even lead to spiral-like conformations due to an uneven distribution of side chains with respect to the backbone.[33,34]

Because so many experimental observations are based on 2d AFM observations and because thin films are extremely important in their own right, it seems of considerable interest to study this situation in detail using computer simulations. In a previous publication the influence of confinement on the persistence length of comb copolymer brushes with flexible side chains involving excluded volume interactions only was addressed.[14] In contrast to the 3d situation a strong increase of λ/D with the side chain length M was observed. As a result of the much stronger excluded-volume effect the scaling regime is reached at a much shorter side chain length than in the 3d case. Here we will continue this investigation and focus on the influence of the competition between excluded volume interactions and attractive interactions between side chains on the comb copolymer conformations. On the one hand, the excluded volume interactions alone lead to very stiff structures, whereas, on the other hand, the attraction may lead to a collapsed structure. We will consider stiff side chains, since these are known to lead to even stiffer bottle-brush structures than do flexible side chains.[15]

The organization of the paper is as follows. In the first section we will combine rigid side chains with a rigid backbone and address the side-chain collapse onto the backbone. Then we consider a flexible backbone and compare the case where flipping of side chains from one side of the backbone to the other is allowed from the case where this is not allowed.

2 Model and Simulation Method

We consider two-dimensional off-lattice comb copolymers with rigid side chains. The comb copolymers are modeled as a collection of spherical beads. The backbone consists of a linear chain of beads connected by bonds such that the bonded spheres just touch. Simulations are performed for comb copolymers with a flexible backbone and a rigid backbone. Every other backbone bead carries a side chain. A side chain consists of a straight chain of tangent spheres with all bond angles equal to 180°. The same holds for the rigid backbone. In the case of a flexible backbone we will distinguish two cases: the non-flipping case where successive side chains are at alternating sides of the backbone and the flipping case where the side chains are free to flip from one side of the backbone to the other. The side chains are connected to the backbone in such a way that the first bead of the side chain acts as a hinge for the rest of the side-chain (Figure 1). The bond between the backbone bead and the first side-chain bead represents a kind of spacer. In this way the side chain has considerably more freedom compared to the case where the backbone grafting bead is used as the hinge.

All beads interact via excluded-volume interactions: beads are not allowed to overlap. Furthermore, the side-chain beads attract each other via a short range attractive potential $V(r) = -\varepsilon/r^6$, where r is the distance between the centers of the beads. The specific form of the potential is, of course, arbitrary; the main point is that it is sufficiently short-ranged.

The side chains at the ends of the backbone have much more freedom to move than side chains near the middle of the backbone. This gives rise to end effects which are considerable for the size of molecules used in our simulations. For a straight backbone these end effects can be easily eliminated using periodic boundary conditions in the direction of the backbone. For a flexible backbone, periodic boundary conditions are inappropriate. In that case care has been taken to exclude the end parts of the brush in the calculation of the relevant conformational properties.

Conformations are generated using Monte Carlo sampling employing the Metropolis criterion. Several types of Monte Carlo moves have been used. Side chains are moved by rotation around the hinge point or by simply choosing a new orientation in an isotropic way. In the case of a flexible backbone, pivot moves and shifts were used. A pivot move consists of choosing one of the backbone beads as the center of rotation and rotating the backbone section between the pivot point and the backbone end over a randomly chosen angle. All side chains connected to this backbone section are rotated in a concerted manner. A shift move is similar, but consists of translating instead of rotating the backbone section and all connected side chains. If flipping is allowed, flip moves are also used. These consist of choosing two backbone beads and mirroring the section of the backbone plus connected side chains in between these beads with respect to the line connecting these beads. Figure 2 illustrates all possible moves.

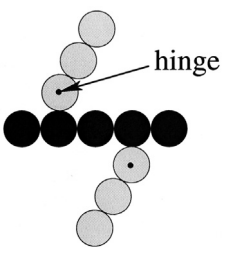

Figure 1. Hinge for side chain rotation.

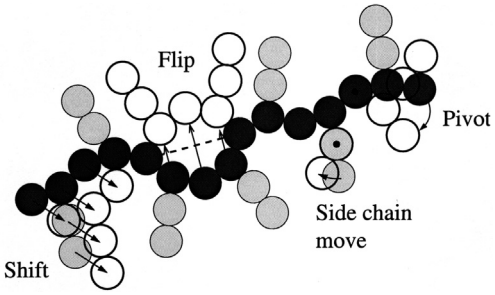

Figure 2. Illustration of the different moves applied. Black spheres represent backbone beads, grey spheres represent side chain beads. White beads represent beads after a move.

3 Results and Discussion

The excluded-volume interaction between side chains is responsible for the worm-like chain character of comb copolymer brushes. The largest stiffness is obtained for strongly adsorbed comb copolymers with rigid side chains. Both the 2d confinement and the rigidity of the side chains enhance the persistence length of the backbone used as a measure of the induced stiffness. To determine this persistence length, the bond angle correlation function, defined as the average cosine, $\langle \cos\theta(s) \rangle$, of the angle between chain segments separated by a distance s along the backbone, was calculated. Figure 3 shows the result on a semilogarithmic scale for a flexible backbone of 128 beads with 64 rigid side chains of length 8 pointing alternately to opposite directions. Only excluded-volume interactions are present. The figure demonstrates that the placement of successive side chains to opposite sides of the backbone creates a strong modulo 4 effect on $\langle \cos\theta(s) \rangle$. Therefore, in the next figure we present the same data together with those for side chain lengths of 4 and 16 for s-values that differ by multiples of 4. All three curves show the same strong decline of the correlation for small values of s, thus confirming the local length scale flexibility of the backbone. Although not presented here,

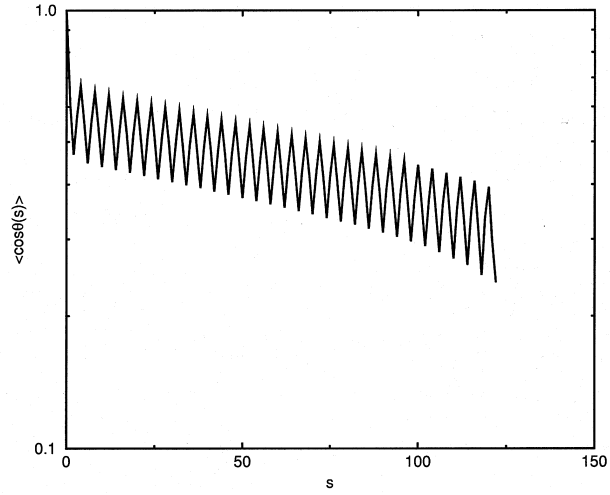

Figure 3. Bond-angle correlation function $\langle \cos\theta(s) \rangle$ of the flexible backbone of two-dimensional polymer brushes with rigid side chains of length 8. The molecules consist of a backbone of 128 beads and 64 side chains pointing alternately to opposite sides of the backbone.

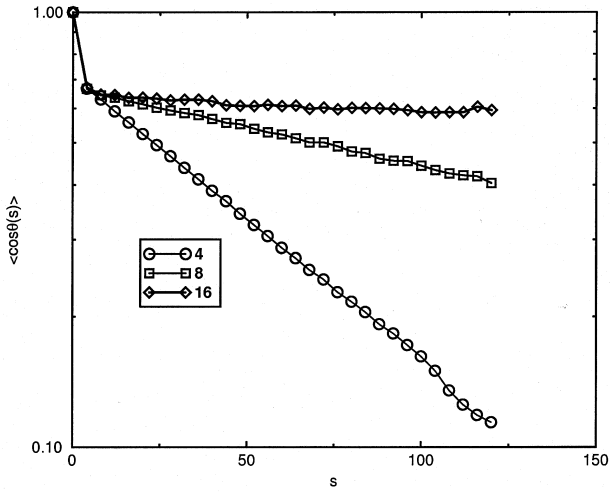

Figure 4. Bond-angle correlation function $\langle \cos\theta(s) \rangle$ of the flexible backbone of two-dimensional polymer brushes with rigid side chains of length 4, 8 and 16. The molecules consist of a backbone of 128 beads and 64 side chains pointing alternately to opposite sides of the backbone. The points correspond to values of s that are multiples of 4.

the value of $\langle \cos\theta(1) \rangle$ is the same for all three side-chain lengths, demonstrating that the spatial distance between successive grafting points is indeed independent of the side-chain length. At larger values of s ($s \geq 8$) a linear behavior in the semilogarithmic presentation (Figure 4) is found. Such a linear behavior is characteristic for a large length scale persistence behavior of the backbone. The persistence length λ is defined by the relation

$$\langle \cos\theta(s) \rangle \propto \exp(-s/\lambda) \tag{1}$$

The next figure (Figure 5) presents the persistence length as a function of the side chain length M for the

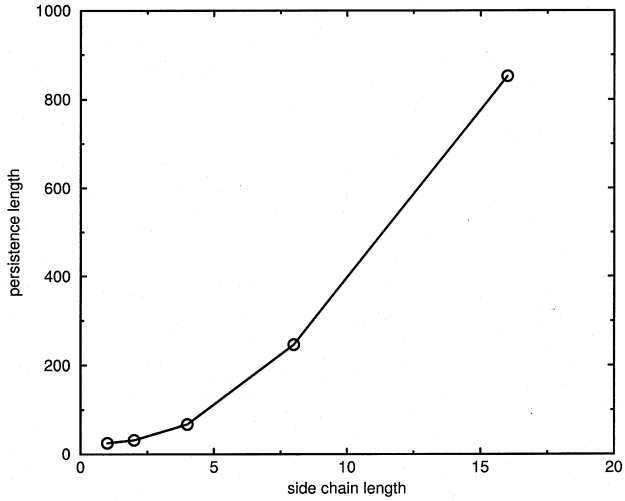

Figure 5. Persistence length λ of two-dimensional polymer brushes as a function of the length of the rigid side chains. The molecules consist of a flexible backbone of 128 beads and 64 side chains pointing alternately to opposite sides of the backbone.

case of a flexible backbone of length 128 with every other bead carrying a rigid side chain pointing alternately to opposite sides of the backbone. For the longest side chains of $M = 16$, the persistence length is already $\cong 850$ in units of the bead size. In comparison, for the case of a 2d comb copolymer brush with flexible side chains of the same length $M = 16$, a value of $\cong 70$ was found.[14]

3.1 Rigid Backbone

In a previous paper[8] the problem of strongly adsorbed comb copolymers with mutually attracting rigid side chains was addressed theoretically. Because the excluded volume effect induces an extreme stiffness for sufficiently long side chains, first a more simplified model was considered by assuming the backbone to be completely rigid. In that case the mean-field analysis demonstrated a second order transition from side chains being oriented preferably perpendicular to the backbone for weak attractions to side chains being collapsed onto the backbone in the strong attraction limit. The results of the corresponding simulations are presented in Figures 6 and 7. Figure 6 presents characteristic snapshots at increasing values of the interaction parameter $\beta = \varepsilon/kT$. The first indications of the presence of collapsed domains, i.e. domains where the side chains are collapsed onto the backbone, appear at $\beta \cong 0.9$. For higher values the collapsed regions increase until around $\beta = 1.1$ the whole system appears collapsed. Figure 7 presents the corresponding distribution functions. For small values of the interaction strength the distribution is as expected monomodal, with a maximum at 90°. At higher values four additional sharp peaks appear, corresponding to the four

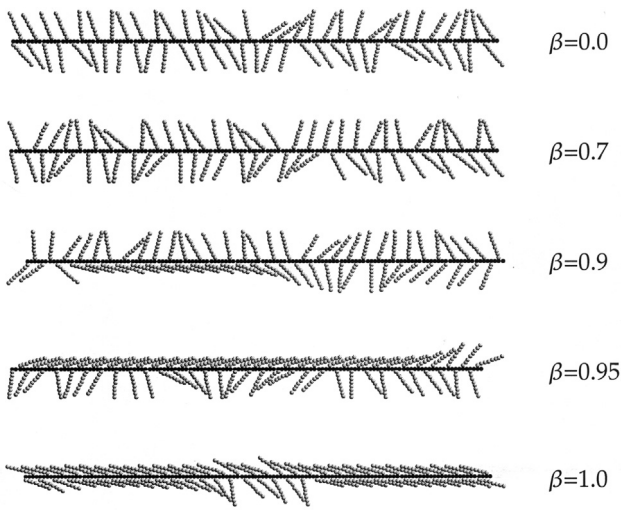

Figure 6. Snapshots of polymer brushes consisting of a rigid backbone of 128 beads with every other bead carrying a rigid side chain of 8 beads pointing alternately to opposite directions of the backbone. Besides the excluded-volume interaction between all beads, the side-chain beads attract each other via a potential $V(r) = -\varepsilon/r^6$ and the snapshots correspond to different values of $\beta = \varepsilon/kT$.

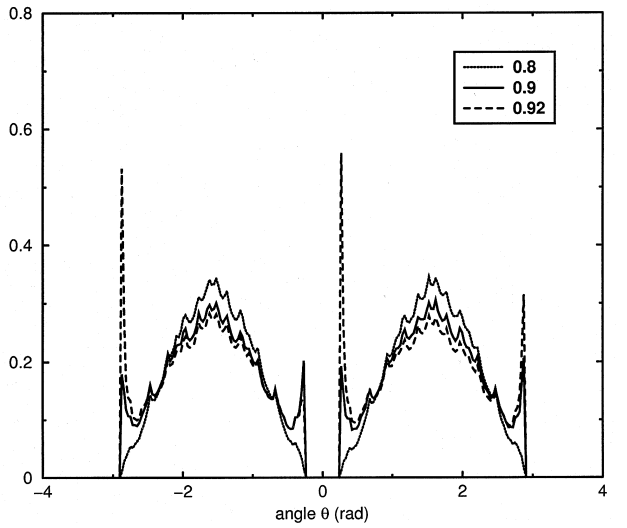

Figure 7. Distribution function for the side-chain orientation as a function of the attraction strength between the side-chain beads for a polymer brush consisting of a rigid backbone of 128 beads, with every other bead carrying a rigid side chain of 8 beads pointing alternately to different sides of the backbone. Besides the excluded-volume interaction between all beads, the side-chain beads attract each other via a potential $V(r) = -\varepsilon/r^6$ and the curves correspond to different values of $\beta = \varepsilon/kT$.

different collapsed states (two at the top side and two at the bottom side of the rigid backbone). The angles of these peaks are determined by

$$\theta = 2 \arcsin\left(\frac{b}{2d}\right) \tag{2}$$

Here b is the bead diameter and d the distance between the grafting points. Once the system is almost completely in one of the collapsed states, it will be quite difficult to reach one of the other collapsed states, since in doing so the system must go through energetically very unfavorable intermediate states. This results in ergodicity problems for large interaction strengths and hence in peaks of different height in the distribution function determined in the simulations. Inside the transition region the distribution function is characterized by the presence of a broad peak centered at 90° corresponding to the non-collapsed state together with the peaks corresponding to the collapsed state. The transition is highly co)operative since the "near" collapse of one side chain requires the participation of several successive side chains. Hence, the initiation or nucleation step for the collapse is much more difficult than the propagation step. In this respect, the transition resembles the well-known helix-coil transition. The simulation data indicate that most of the transition takes place in the interval $\beta \in [0.9 - 1.0]$.

3.2 Flexible Backbone

Next we remove the rigidity constraint from the backbone. We will distinguish separately the case where side chain flipping is allowed and where it is not. In the latter case the side chains point again alternately to opposite sides of the backbone. We start with the latter case.

Figure 8 presents a series of snapshots for side chains of length 8 and values of the interaction parameter up to $\beta = 1.0$. Figure 9 and 10 present $\langle \cos\theta(s=1) \rangle$ and the persistence length λ as a function of β for values up to $\beta = 0.7$. For $\beta = 0$, the case of excluded-volume interaction only, the persistence length is of the order of 245, approximately twice as large as the extended conformation length 128 of the backbone. On increasing the attraction between the side chains, the snapshots reveal no sign of side chain collapse onto the backbone. Rather, the side chains at both sides of the backbone cluster together by local folding of the backbone. This local folding of the backbone is clearly visible in the bond angle correlation functions as a decrease in $\langle \cos\theta(1) \rangle$ for increasing values of β. The preferable orientation of the side chains appears to be perpendicular to the backbone direction. The persistence length of the backbone decreases almost linearly with β (Figure 10), from a value of 245 at $\beta = 0$ to ca. 180 at $\beta = 0.7$. This is in excellent agreement with the theoretical analysis, where by generalizing the results obtained for a rigid backbone to a backbone with finite rigidity, a linear decrease in persistence length with interaction strength was predicted for the so-called weak attraction regime.[8] The weak attraction regime was defined by $\beta \leq \beta^*$, where β^* is the critical interaction strength for the collapse transition in case of a rigid backbone. The attraction energies considered here ($\beta \leq 0.7$) clearly belong to this regime and the computer simulation results therefore nicely support these predictions. Despite

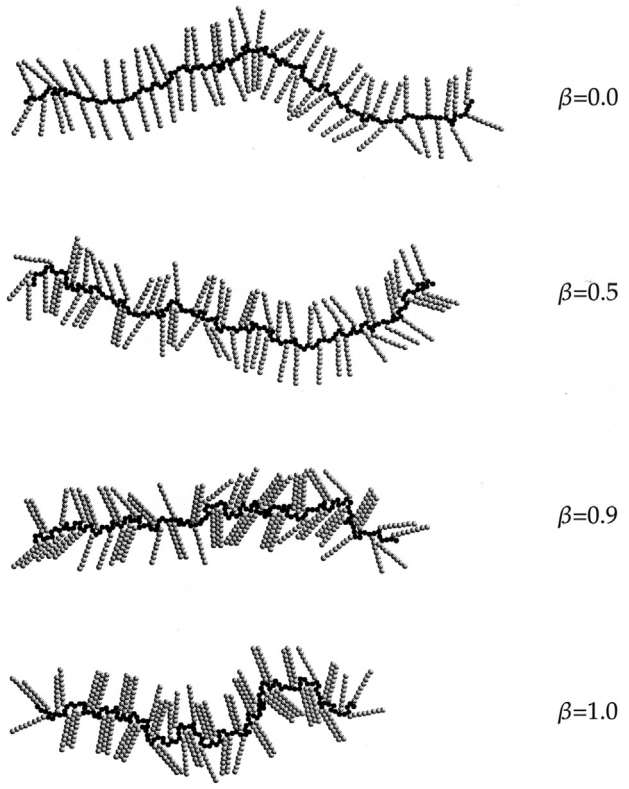

Figure 8. Snapshots of polymer brushes consisting of a flexible backbone of 128 beads with every other bead carrying a rigid side chain of 8 beads pointing alternately to opposite directions of the backbone. Besides the excluded-volume interaction between all beads, the side-chain beads attract each other via a potential $V(r) = -\varepsilon/r^6$ and the snapshots correspond to different values of $\beta = \varepsilon/kT$.

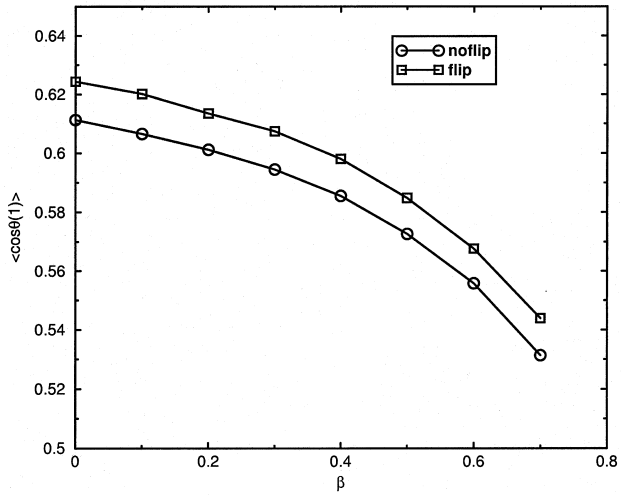

Figure 9. The value of the bond-angle correlation function $\langle \cos\theta(s=1)\rangle$ of the flexible backbones of two-dimensional polymer brushes consisting of a flexible backbone of 128 beads with every other bead carrying a rigid side chain of 8 beads as a function of the attraction strength $\beta = \varepsilon/kT$ between the side chains. Besides the excluded-volume interaction between all beads, the side-chain beads attract each other via a potential $V(r) = -\varepsilon/r^6$. The upper curve corresponds to the case where side chain flipping is allowed (cf. Fig. 11). For the lower curve the side chains point alternatingly to opposite sides of the backbone (cf. Figure 8).

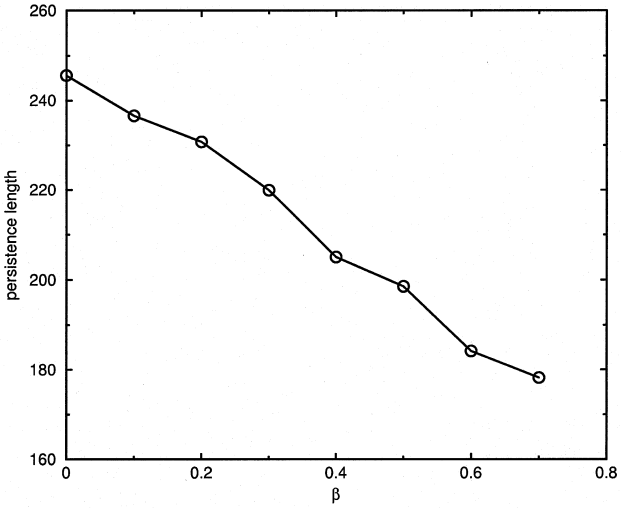

Figure 10. Persistence length λ of two-dimensional polymer brushes consisting of a flexible backbone of 128 beads with every other bead carrying a rigid side chain of 8 beads as a function of the attraction strength $\beta = \varepsilon/kT$ between the side chains. Besides the excluded-volume interaction between all beads, the side chain beads attract each other via a potential $V(r) = -\varepsilon/r^6$. The 64 side chains point alternatingly to opposite sides of the backbone.

the reduction in persistence length, for the size of the molecules considered here the comb copolymer appears essentially as a straight comb copolymer brush.

The situation becomes quite different if flipping of side chains from one side of the backbone to the other side is allowed. Figure 11 presents characteristic snapshots as a function of the interaction strength β. Figure 9 also presents $\langle \cos\theta(s=1)\rangle$ as a function of β for this case. The decrease of $\langle \cos\theta(s=1)\rangle$, characteristic for local shrinking, is similar to the non-flipping case. The absolute value is somewhat larger because conformations where successive side chains point to the same direction of the backbone are now also included. These will locally lead to slightly larger values of $\cos\theta(s=1)$ and hence to a slightly larger value of $\langle \cos\theta(s=1)\rangle$. Figure 12 presents the persistence length as a function of the interaction strength. Already without any attraction between the side chains, the persistence length of the backbone is much smaller compared to the non-flipping case; of the order of 55 compared to 245. This value is already considerably smaller than the length of the extended conformation of the molecules simulated. For increasing strength of the attraction between the side chains, consecutive side chains start to aggregate at one side of the backbone. Hence, alternating sections with side chains preferably at the same side of the backbone are formed. In the intro-

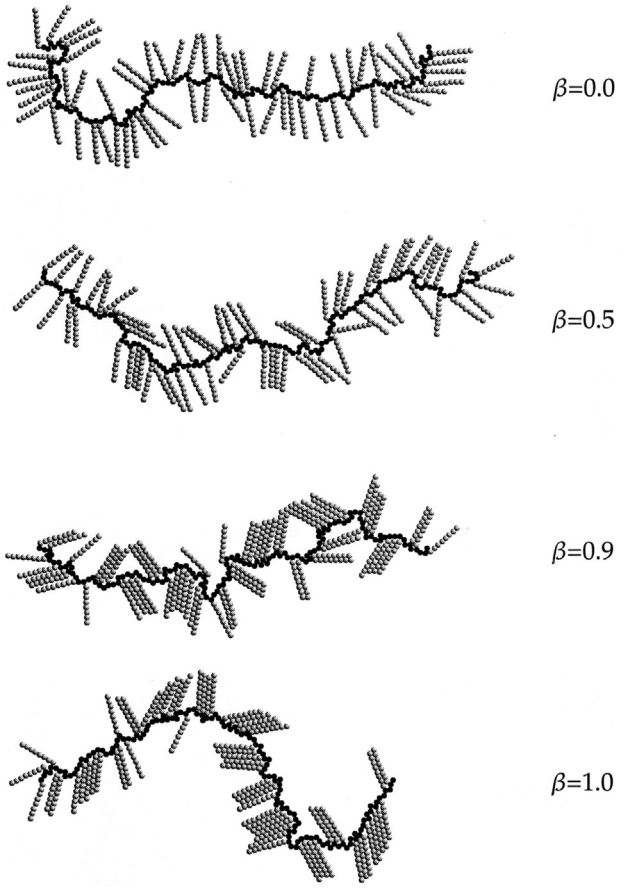

Figure 11. Snapshots of polymer brushes consisting of a flexible backbone of 128 beads with every other bead carrying a rigid side chain of 8 beads. Besides the excluded-volume interaction between all beads, the side-chain beads attract each other via a potential $V(r) = -\varepsilon/r^6$ and the snapshots correspond to different values of $\beta = \varepsilon/kT$. The side chains are free to flip from one side of the backbone to the other.

duction we referred already to the literature demonstrating that an uneven distribution of side chains with respect to the backbone may lead to spiraling conformations.[7, 33, 34] We now see that such an uneven distribution may simply result from attraction between side chains. However, because the uneven distribution pertains to finite domains only rather than to the whole chain, the spiraling results in bending alternately inward and outward (Figure 11). Furthermore, the persistence length again decreases almost linearly with the interaction strength β (Figure 12).

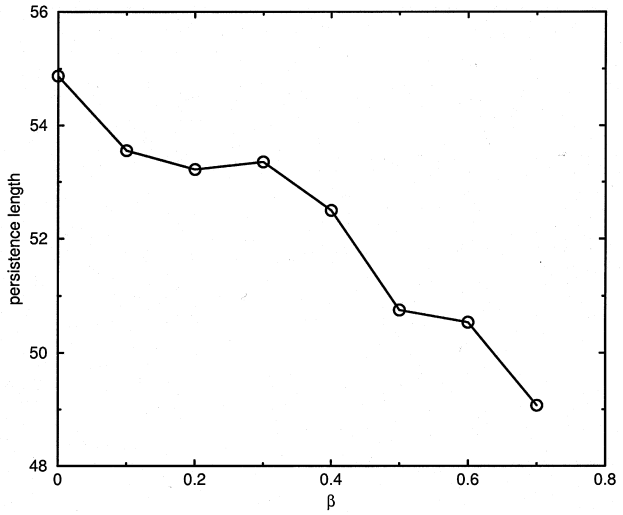

Figure 12. Persistence length λ of two-dimensional polymer brushes consisting of a flexible backbone of 128 beads with every other bead carrying a rigid side chain of 8 beads as a function of the attraction strength $\beta = \varepsilon/kT$ between the side chains. Besides the excluded-volume interaction between all beads, the side-chain beads attract each other via a potential $V(r) = -\varepsilon/r^6$. The 64 side chains can freely flip from one side of the backbone to the other.

confinement, the situation considered in this paper. The presence of an additional attraction between the side chains reduces the persistence length, i.e., the parameter that is used to quantify the stiffness of the backbone. If side-chain flipping is allowed during the preparative stage, domains of equal side chain orientation with respect to the backbone are formed. These domains are formed for an attraction strength that is characteristic for the transition of side chains collapsing onto the backbone in the case of a rigid rod backbone. The presence of these domains results in a characteristic local curvature of the backbone, with side chains pointing to the convex side.

Acknowledgement: Drs. *Valentina Vasilevskaya, Andrei Subbotin, Igor Erukhimovich* and *Roman Stepanyan* are gratefully acknowledged for useful discussions.

Received: April 9, 2002
Revised: June 25, 2002
Accepted: July 11, 2002

4 Conclusions

Comb copolymers with a flexible backbone and a high density of side chains have a characteristic stiff cylindrical brush structure due to the excluded volume interactions between the side chains. This effect is strongly enhanced by using stiff side chains and two-dimensional

[1] T. M. Birshtein, O. V. Borisov, E. B. Zhulina, A. R. Khokhlov, T. A. Yurasova, *Polym. Sci. U.S.S.R.* **1987**, *29*, 1293.
[2] Z.-G. Wang, S. A. Safran, *J. Chem. Phys.* **1988**, *89*, 5323.
[3] G. H. Fredrickson, *Macromolecules* **1993**, *26*, 2825.
[4] Y. Rouault, O. V. Borisov, *Macromolecules* **1996**, *29*, 2605.

[5] A. Subbotin, M. Saariaho, O. Ikkala, G. ten Brinke, *Macromolecules* **2000**, *33*, 3447.
[6] A. Subbotin, M. Saariaho, R. Stepanyan, O. Ikkala, G. ten Brinke, *Macromolecules* **2000**, *33*, 6168.
[7] I. I. Potemkin, A. R. Khokhlov, P. Reineker, *Eur. Phys. J. E* **2001**, *4*, 93.
[8] R. Stepanyan, A. Subbotin, G. ten Brinke, *Phys. Rev. E* **2001,** *63, 61805.*
[9] R. Stepanyan, A. Subbotin, G. ten Brinke, *Macromolecules* **2002**, in press.
[10] Y. Nakamura, T. Norisuye, *Polym. J.* **2001**, *33*, 874.
[11] M. Saariaho, O. Ikkala, I. Szleifer, I. Erukhimovich, G. ten Brinke, *J. Chem. Phys.* **1997**, *107*, 3267.
[12] G. ten Brinke, O. Ikkala, *TRIP* **1997**, *5*, 213.
[13] Y. Rouault, *Macromol. Theory Simul.* **1998**, *7*, 395.
[14] M. Saariaho, O. Ikkala, G. ten Brinke, *J. Chem. Phys.* **1999**, *110*, 1180.
[15] M. Saariaho, A. Subbotin, I. Szleifer, O. Ikkala, G. ten Brinke, *Macromolecules* **1999**, *32*, 4439.
[16] M. Saariaho, A. Subbotin, O. Ikkala, G. ten Brinke, *Macromol. Rapid Commun.* **2000**, *21*, 110.
[17] Y. Tsukahara, K. Mizuno, A. Segawa, Y. Yamashita, *Macromolecules* **1989**, *22*, 1546.
[18] Y. Tsukahara, K. Tsutsumi, Y. Yamashita, *Macromolecules* **1989**, *22*, 2869.
[19] Y. Tsukahara, K. Tsutsumi, Y. Yamashita, S. Shimada, *Macromolecules* **1990**, *23*, 5201.
[20] M. Mishra, "*Macromolecular Design: Concept and Practice*", Polymer Frontiers International Inc., New York 1993.
[21] K. L. Beers, G. G. Scott, K. Mattyjaszewski, S. S. Sheiko, M. Möller, *Macromolecules* **1998**, *31*, 9413.
[22] M. Schappacher, C. Billaud, C. Paulo, A. Deffieux, *Macromol. Chem. Phys.* **1999**, *200*, 2377.
[23] H. G. Boerner, K. Beers, K. Matyjaszewski, S. S. Sheiko, M. Möller, *Macromolecules* **2001**, *34*, 4375.
[24] M. Wintermantel, M. Schmidt, Y. Tsukahara, K. Kajiwara, S. Kohjiya, *Macromol. Rapid Commun.* **1994**, *15*, 279.
[25] M. Wintermantel, K. Fisher, M. Gerle, R. Ries, M. Schmidt, K. Kajiwara, H. Urakawa, I. Wataoka, *Angew. Chem. Int. Ed. Engl.* **1995**, *34*, 1472.
[26] M. Wintermantel, M. Gerle, K. Fischer, M. Schmidt, I. Wataoka, H. Urakawa, K. Kajiwara, Y. Tsukahara, *Macromolecules* **1996**, *29*, 978.
[27] P. Dziezok, S. S. Sheiko, K. Fischer, M. Schmidt, M. Möller, *Angew. Chem. Int. Ed. Engl.* **1997**, *36*, 2812.
[28] S. S. Sheiko, M. Gerle, K. Fisher, M. Schmidt, M. Möller, *Langmuir* **1997**, *13*, 5368.
[29] K. Fischer, M. Schmidt, *Macromol. Rapid. Commun.* **2001**, *22*, 787.
[30] M. Gerle, K. Fischer, S. Roos, A. H. E. Müller, M. Schmidt, S. S. Sheiko, S. Prokhorova, M. Möller, *Macromolecules* **1999**, *32*, 2629.
[31] S. S. Sheiko, *Adv. Polym. Sci.* **2000**, *151*, 61.
[32] S. S. Sheiko, S. A. Prokhorova, K. L. Beers, K. Matyjaszewsky, I. I. Potemkin, A. R. Khokhlov, M. Möller, *Macromolecules* **2001**, *34*, 8354.
[33] P. G. Khalatur, A. R. Khokhlov, S. A. Prokhorova, S. S. Sheiko, M. Möller, P. Reineker, D. G. Shirvanyanz, N. Yu. Starovoitova, *Eur. Phys. J. E* **2000**, *1*, 99.
[34] P. G. Khalatur, D. G. Shirvanyanz, N. Yu. Starovoitova, A. R. Khokhlov, *Macromol. Theory Simul.* **2000**, *9*, 141.